Physics of Semiconductors. Computational materials science

UDC 538.9

EDN WANXEA
https://www.doi.org/10.33910/2687-153X-2025-6-2-104-109

The effect of uniaxial compression on micro- and macro-parameters of CdSe quantum dots of different sizes

Yu. A. Melchakova [1,2] ✉, A. I. Solomonov [1]

[1] National Research University ITMO, 49 Kronverksky Ave., Saint Petersburg 197101, Russia
[2] Tomsk State University, 36 Lenin Ave., Tomsk 634050, Russia

Authors

Yulia A. Melchakova, ORCID: 0000-0003-4694-2995, e-mail: iuliia.melchakova@metalab.ifmo.ru

Alexander I. Solomonov, ORCID: 0000-0003-1348-5951

For citation: Melchakova, Yu. A., Solomonov, A. I. (2025) The effect of uniaxial compression on micro- and macro-parameters of CdSe quantum dots of different sizes. *Physics of Complex Systems*, 6 (2), 104–109. https://www.doi.org/10.33910/2687-153X-2025-6-2-104-109 EDN WANXEA

Received 21 February 2025; reviewed 1 April 2025; accepted 1 April 2025.

Funding: This work was supported by the Ministry of Education and Science of the Russian Federation under the state assignment (No. FSWM-2025-0007).

Abstract. In this paper, we analyze and discuss DFT calculations for zinc blende and wurtzite CdSe quantum dots (QDs). We found QDs with a size of 1.6 Å to be stable and relaxed using the PBE exchange-correlation functional. The behavior of frontier orbitals (HOMO, LUMO) was examined for an unrelaxed structure to include symmetry and degeneracy. The results of the Purcell factor of the zinc blende and wurtzite QDs with a size of 1.6 Å were found to be stable under axial compression. The designed quantum dots demonstrate mechanical and optical stability, their properties retained under uniaxial compression.

Keywords: DFT, FDTD, quantum dots, cadmium selenide, wurtzite, zinc blende, electronic properties, Purcell factor

Introduction

CdSe quantum dots are semiconductor nanocrystals that exhibit unique optical and electronic properties due to their small size and quantum confinement effects (Alnemrat et al. 2014; Huang et al. 2024; Kolobkova et al. 2024; Zhang et al. 2024a; 2024b). These quantum dots possess a wide range of properties, including size-dependent optical ones such as a size-dependent band gap (Alsalme et al. 2025; Askirka et al. 2025; Memon et al. 2025). As their size goes down, the band gap increases, which induces a shift in the absorption and emission spectra (Alnemrat et al. 2014). This results in the emission of light at different wavelengths (colors) based on the quantum dot size. The electronic and optical properties of CdSe quantum dots are governed by the quantum confinement effect, where the motion of electrons and holes is restricted in all three spatial dimensions, leading to discrete energy levels (Shabaev et al. 2012). This gives rise to unique optical phenomena like fluorescence and tunable emission, which can be adjusted by altering the size of the dots.

CdSe quantum dots often have a high quantum yield and photoluminescence efficiency, which makes them excellent for light-emitting applications such as displays and sensors (Magaryan et al. 2016; Silva 2014; Zhang et al. 2024a). CdSe quantum dots exhibit tunable absorption and emission spectra, which can be fine-tuned by adjusting their size during synthesis. This makes them versatile for various applications.

Tuning the optical properties of CdSe QDs through uniaxial compression is a fascinating approach that leverages mechanical stress to induce changes in the electronic and optical behavior of these nanomaterials (Gong et al. 2016; Pisheh et al. 2017; Rodríguez-Magdaleno et al. 2022). Size-dependent band

gap behavior means that applying strain can effectively tune the frontier states of the quantum dots, leading to changes in their absorption and emission spectra. Strain can alter the electronic band structure, i. e. degeneracy, polarization, and band gap value by affecting the overlap of electron and hole wavefunctions in the QDs. This modification changes the exciton binding energy, which is the energy required to separate the electron–hole pair.

Compressive strain can also induce changes in the valence band and conduction band alignment and localization, modifying the optical absorption spectrum (Rodríguez-Magdaleno et al. 2022). The application of uniaxial strain can shift the absorption edge (onset of absorption) to different energies based on strain direction, magnitude, and quantum dot shape. This will result in a change in the wavelengths at which QDs absorb light. The fluorescence emission spectrum may be red-shifted or blue-shifted depending on the specific strain applied. Compressing QDs along a certain axis, for example, might reduce the band gap, causing a red shift in the emission.

Computational section

The electronic structure calculations of low-dimensional crystalline lattices were performed using Vienna Ab-initio Simulation Package (VASP) (Kresse, Furthmüller 1996; Kresse, Hafner 1993; 1994; Kresse, Joubert 1999) within Density Functional Theory (DFT) (Kohn, Sham 1965). A plane-wave basis set coupled with the projector augmented wave (PAW) method (Blöchl 1994; Kresse et al. 1999), GGA-PBE (Perdew et al. 1996) functional, and Grimme D3 correction (Grimme 2006) for van-der-Waals interaction were used in the study. Optimization and single point calculations were made only at Γ point due to an absence of periodicity. For all elements involved in the electronic structure calculations, PAW potentials were used. Twelve and six outer electrons were treated as valence electrons for cadmium and selenium respectively. A vacuum interval of 20 Å was set along 3 axes to avoid artificial interactions between adjacent unit cell images. In all calculations, the cut-off energy was equal to 500 eV. During optimization, the maximum force acting on atoms less than 0.001 eV/Å was used as a stopping criterion for structural minimization.

The Purcell factor calculations were performed using the Finite Difference Time Domain (FDTD) method. Three independent orthogonally-oriented dipole sources were placed at the center of the nanoparticle. For each dipole, the Purcell factor was calculated as the ratio between the power radiated in the environment with a nanoparticle and the power radiated in free space. After three independent calculations for orthogonal sources, the final Purcell factor was averaged.

Results

The optimization procedure involved refining the atomic positions to minimize residual forces. Bulk CdSe crystals in both the wurtzite and zinc blende phases were obtained from the Crystallography Open Database and optimized using periodic boundary conditions (PBC) within Density Functional Theory (DFT). Subsequently, spherical regions with a radius of 8 Å were extracted from the bulk (see Fig. 1). These regions were then further optimized to adjust the atomic coordinates and correct for any dangling bonds at the surface.

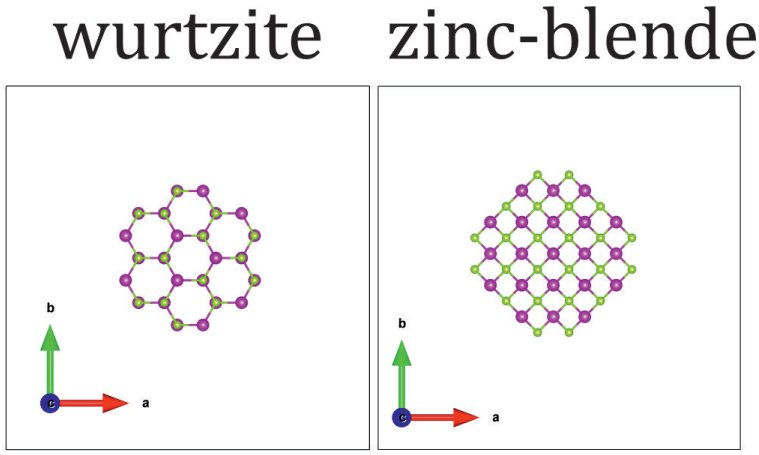

Fig. 1. Structure of wurtzite and zinc-blende CdSe quantum dots. Cd and Se atoms are shown in purple and green respectively

The optimized structure of the wurtzite CdSe quantum dot is illustrated in Fig. 2. The outer shell, which consisted of both Cd and Se atoms, was subjected to relaxation during the optimization procedure. Thus, reduction of symmetry to the C1 point group is an expected result due to the formation of dangling bonds with the following outer shell relaxation; nevertheless, the quantum dot retains its spherical shape, thereby confirming its structural stability.

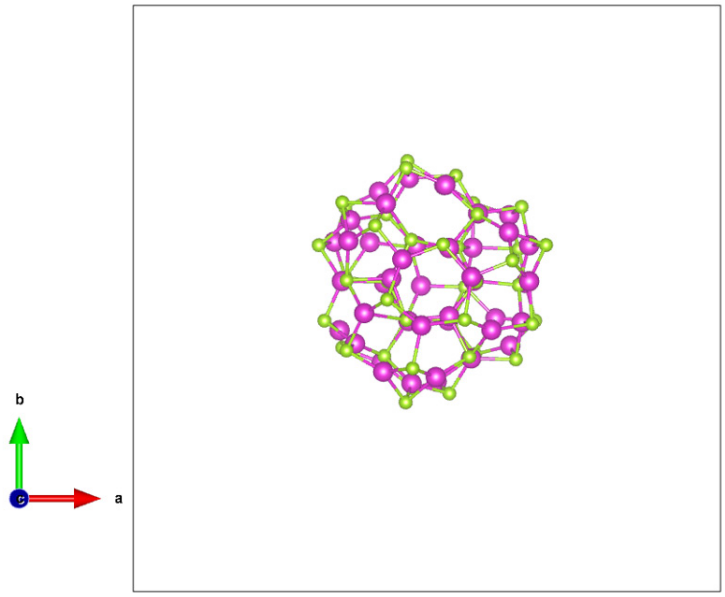

Fig. 2. Structure of the optimized wurtzite CdSe quantum dots. Cd and Se atoms are shown in purple and green respectively

The electronic properties of spherical wurtzite CdSe were investigated using both pure and hybrid functionals, specifically PBE and HSE06 (Fig. 3). Both computational approaches indicated the semiconducting nature of the material; however, the HSE06 calculations predicted a band gap approximately twice as large (2.17 eV) as the value obtained from the PBE functional (1.15 eV). While pure functionals are known to generally underestimate band gap values, the shapes of the density of states (DOS) peaks were found to be accurately reproduced, making them suitable for tracking general patterns in the system.

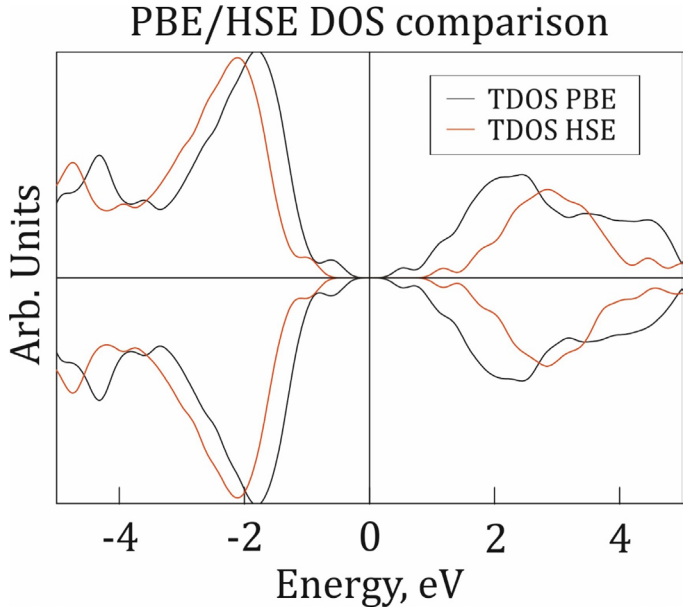

Fig. 3. Density of the states of wurtzite CdSe quantum dots calculated by PBE (black lines) and HSE06 (red lines) functionals. Fermi level assigned to 0 eV

 https://www.doi.org/10.33910/2687-153X-2025-6-2-104-109

Axial compression and extension were then examined. Two additional structures, each with a 10% deformation, were created and optimized, as shown in Fig. 4. The extended CdSe quantum dot was generated by extension along the *xy*-plane, while the compressed CdSe quantum dot was formed by compression in the *xy*-plane. Despite these deformations, the symmetry of the quantum dots remained C1 and was preserved throughout the optimization process.

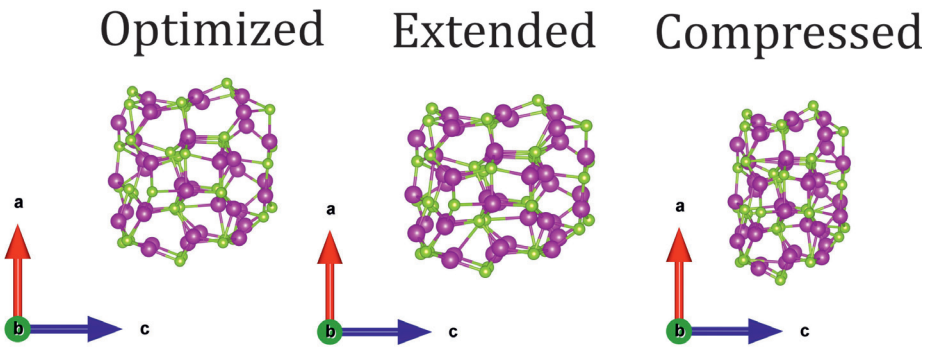

Fig. 4. Optimized, extended and compressed wurtzite CdSe quantum dots. Cd and Se atoms are shown in purple and green respectively

The impact of axial deformations of DOS was examined further. DOS calculations (Fig. 5) demonstrated the shift of the occupied states closer to the Fermi level and no change in the band gap value. The QD extension would lead to a shift of vacant states lower to the Fermi level contrary to the compression case. The distorted structure can be characterized by diffuse localization of states around –2 and 2 eV in comparison with the pristine model.

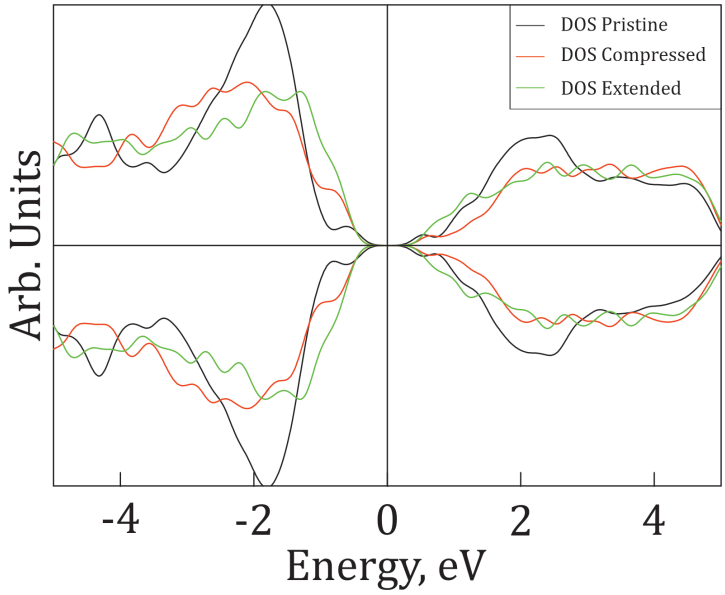

Fig. 5. Total density of states (TDOS) of pristine, compressed, and extended CdSe QDs. TDOS of the pristine lattice is shown with black curves, with TDOS of compressed and extended CdSe QDs marked with red and green curves respectively

To proceed further, we evaluate the Purcell effect spectra under the deformation parameter. In the Finite Difference Time Domain, we simulate an ellipsoid particle with a major axis radius R_{major} = 8 Å and a different minor axis R_{minor} changing from $0.9R_{major}$ to R_{major}. We placed at the center three orthogonal dipole sources and the average final factor and calculated the average final factor.

Fig. 6 shows the average Purcell effect for zinc-blende (left) and wurtzite (right) phases of the CdSe. For the wurtzite phase, we observe a monotonically increased Purcell factor with an increased wavelength. A similar pattern can be also observed in the zinc-blende phase. Besides, the cubic phase shows a narrow

peak at a wavelength of 580 nm. The impact of axial deformation was examined. The Purcell factor for both phases showed stability of the properties under a 10% deformation.

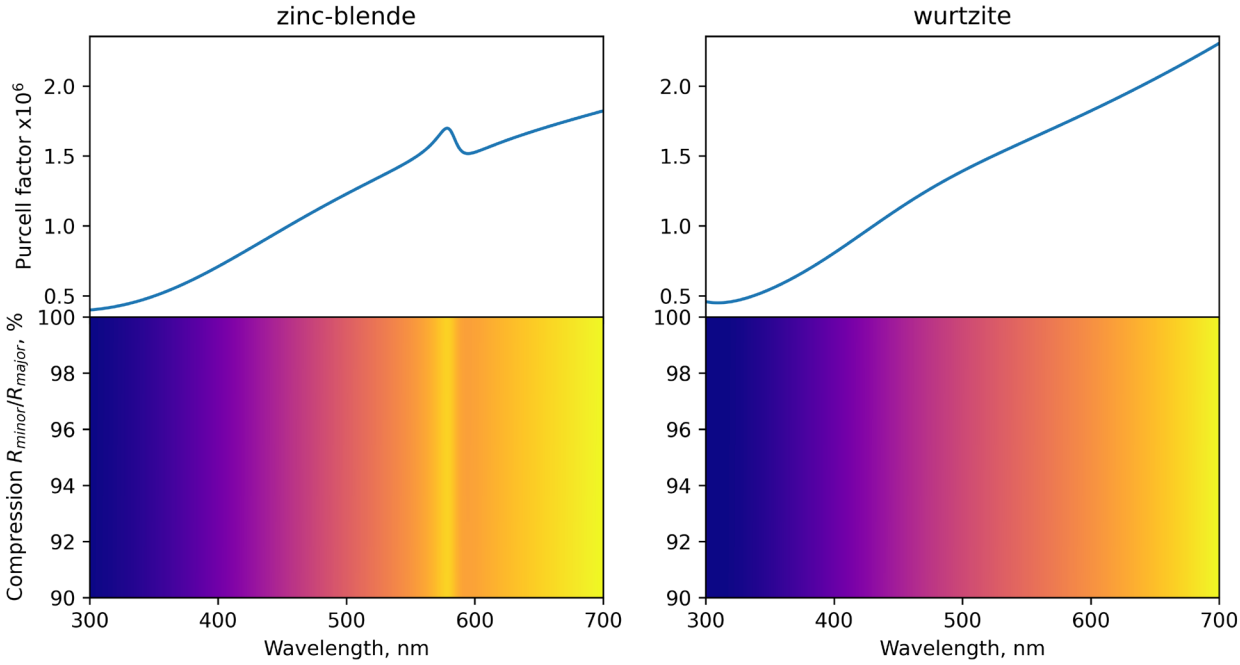

Fig. 6. Purcell factor of CdSe QDs with compression dependence

Conclusions

This paper analyzed and discussed the impact of extension and compression of the CdSe quantum dot of zinc blende and wurtzite phases. We found that for small-sized CdSe QDs, the strain and compression effect do not lead to conductivity properties and a band gap decrease. Theoretical modelling predicts the stability of the 1.6 Angstrom QD and its semiconductor properties with a band gap of about 2eV. Designed quantum dots demonstrate mechanical and optical stability, their properties retained under uniaxial compression.

Conflict of Interest

The authors declare that there is no conflict of interest, either existing or potential.

Author Contributions

Yu. Melchakova: DFT calculations and modelling, manuscript writing, conceptualization.
A. Solomonov: FDTD calculations and modelling, manuscript writing.

Acknowledgements

The authors would like to extend their gratitude to Professor Anna Rodina for her significant contribution to the conceptualization of the manuscript and fruitful discussions throughout the research.

Yu. M. expresses gratitude to Information Technology Centre, Novosibirsk State University, for providing access to a supercomputer and expresses gratitude to ITMO Fellowship program for the financial support.

References

Alnemrat, S., Park, Y. H., Vasiliev, I. (2014) Ab initio study of ZnSe and CdTe semiconductor quantum dots. *Physica E: Low-dimensional Systems and Nanostructures*, 57, 96–102. https://doi.org/10.1016/j.physe.2013.10.037 (In English)

Alsalme, A., Eltawil, M. A., Alsaeedi, H. et al. (2025) Enhancing the photocatalytic efficiency of g-C3N4 by sonochemical dispersion of CdSe quantum dots for photocatalytic degradation of industrial organic pollutants under commercial light source. *Materials Chemistry and Physics*, 334, article 130367. https://doi.org/10.1016/j.matchemphys.2025.130367 (In English)

Askirka, V., Stsiapura, V., Miluski, P. (2025) Efficient FRET in new co-doped Tb(tmhd)3-CdSe/ZnS quantum dots-poly (methyl methacrylate) polymer nanocomposites for optoelectronic and sensor applications. *Journal of Luminescence*, 279, article 121047. https://doi.org/10.1016/j.jlumin.2024.121047 (In English)

Blöchl, P. E. (1994) Projector augmented-wave method. *Physical Review B*, 50 (4), 17953–17979. https://doi.org/10.1103/PhysRevB.50.17953 (In English)

Gong, K., Beane, G., Kelley, D. F. (2016) Strain release in metastable CdSe/CdS quantum dots. *Chemical Physics*, 471, 18–23. https://doi.org/10.1016/j.chemphys.2015.09.009 (In English)

Grimme, S. (2006) Semiempirical GGA-type density functional constructed with a long-range dispersion correction. *Journal of Computational Chemistry*, 27 (15), 1787–1799. https://doi.org/10.1002/jcc.20495 (In English)

Huang, X., Li, N., Kim, K-H., Chang, Q. et al. (2024) Enhancing luminescence efficiency of CdSe quantum dots through the amine-assisted Z-type ligand. *Cell Reports Physical Science*, 5 (11), article 102268. https://doi.org/10.1016/j.xcrp.2024.102268 (In English)

Kohn, W., Sham, L. J. (1965) Self-consistent equations including exchange and correlation effects. *Physical Review B*, 140 (4A), A1133–A1138. https://doi.org/10.1103/PhysRev.140.A1133 (In English)

Kolobkova, E. V., Nikonorov, N. V., Kuznetsova, M. S., Bataev, M. N. (2024) Controlling the luminescence of CdSe quantum dots in the fluorinephosphate glass. *Journal of Non-Crystalline Solids*, 646, article 123248. https://doi.org/10.1016/j.jnoncrysol.2024.123248 (In English)

Kresse, G., Furthmüller, J. (1996) Efficient iterative schemes for ab initio total-energy calculations using a plane-wave basis set. *Physical Review B*, 54 (16), 11169–11186. https://doi.org/10.1103/PhysRevB.54.11169 (In English)

Kresse, G., Hafner, J. (1993) Ab initio molecular dynamics for liquid metals. *Physical Review B*, 47 (1), 558–561. https://doi.org/10.1103/PhysRevB.47.558 (In English)

Kresse, G., Hafner, J. (1994) Ab initio molecular-dynamics simulation of the liquid-metal–amorphous-semiconductor transition in germanium. *Physical Review B*, 49 (20), 14251–14269. https://doi.org/10.1103/PhysRevB.49.14251 (In English)

Kresse, G., Joubert, D. (1999) From ultrasoft pseudopotentials to the projector augmented-wave method. *Physical Review B*, 59 (3), 1758–1775. https://doi.org/10.1103/PhysRevB.59.1758 (In English)

Magaryan, K. A. Mikhailov, M. A., Karimullin, K. R. et al. (2016) Spatially-resolved luminescence spectroscopy of CdSe quantum dots synthesized in ionic liquid crystal matrices. *Journal of Luminescence*, 169, 799–803. https://doi.org/10.1016/j.jlumin.2015.08.064 (In English)

Memon, R., Shaheen, I., Qureshi, A., Niazi, J. H. (2024) Enhanced detection of cardiac troponin-I using CdSe/CdS/ZnS core-shell quantum dot/TiO2 heterostructure photoelectrochemical sensor. *Journal of Alloys and Compounds*, 1008, article 176592. https://doi.org/10.1016/j.jallcom.2024.176592 (In English)

Perdew, J. P., Burke, K., Ernzerhof, M. (1996) Generalized gradient approximation made simple. *Physical Review Letters*, 77 (18), 3865–3868. https://doi.org/10.1103/PhysRevLett.77.3865 (In English)

Pisheh, H. S., Gheshlaghi, N., Ünlü, H. (2017) The effects of strain and spacer layer in CdSe/CdS/ZnS and CdSe/ZnS/CdS core/shell quantum dots. *Physica E: Low-dimensional Systems and Nanostructures*, 85, 334–339. https://doi.org/10.1016/j.physe.2016.07.007 (In English)

Rodríguez-Magdaleno, K. A., Pérez-Álvarez, R., Ungan, F., Martínez-Orozco, J. C. (2022) Strain effect on the intraband absorption coefficient for spherical CdSe/CdS/ZnSe core–shell–shell quantum dots. *Materials Science in Semiconductor Processing*, 141, article 106400. https://doi.org/10.1016/j.mssp.2021.106400 (In English)

Shabaev, A., Rodina, A. V., Efros, A. L. (2012) Fine structure of the band-edge excitons and trions in CdSe/CdS core/shell nanocrystals. *Physical Review B*, 86 (20), article 205311. https://doi.org/10.1103/PhysRevB.86.205311 (In English)

Silva, A. C. A., Vieira de Deus, S. L., Silva, M. J. B, Dantas, N. O. (2014) Highly stable luminescence of CdSe magic-sized quantum dots in HeLa cells. *Sensors and Actuators B: Chemical*, 191, 108–114. https://doi.org/10.1016/j.snb.2013.09.063 (In English)

Zhang, Y., Shida, L., Yanshen, Z. et al. (2024b) Promoting photoelectric performance through extraction of hot electron from Cu-doped CdSe quantum dots. *Journal of Alloys and Compounds*, 1005, article 176037. https://doi.org/10.1016/j.jallcom.2024.176037 (In English)

Zhang, Y., Wenchao, L., Like, L. (2024a) Optical fiber fluorescence Cu2+ sensing technology based on CdSe/ZnS quantum dots: Large detection range, low detection limit. *Analytica Chimica Acta*, 1331, article 343300. https://doi.org/10.1016/j.aca.2024.343300 (In English)